

# Browsing large graphs with XJS, a graph drawing tool in JavaScript

auth0 and auth1

Institute, US,  
auth0@hotmail.com, auth1@gmail.com,  
X github home page: <https://github.com/X>

**Abstract.** There has been progress in visualization of large graphs recently. Tools appeared that can render a huge graph in seconds. However, if we request that the node labels are readable, and the edges are routed around the nodes, then the problem remains difficult. Interacting with a large graph in a web browser with the same ease as browsing an online map is still a challenging task. In this paper we describe a few novel approaches to large graph visualization that we developed in open-source JavaScript software.

We give a new efficient edge routing algorithm, where the edges are routed around the nodes. The algorithm produces edge paths which are visually appealing and shortest in their homotopy class.

To facilitate graph visualization with WebGL, or any other platform supporting tiles, we propose a new simple and efficient tiling method. The method guarantees that in every view, except of the highest level, the number of visible entities per tile is not larger than a predefined bound.

The edge routing algorithm mentioned above is reused at the tiling stage to simplify the paths on the upper levels.

## Introduction

Our software is open source written in TypeScript, it is consumed as a set of NPM packages. It runs on the client desktop or on a phone, and renders the graph in a web browser. We target large but not huge graphs. The maximum number of vertices of the graphs we applied our tool to was 28k, and the maximum number of the edges was 237k.

We discovered the algorithms described below while studying the imperfections of the previous version of the tool. The findings seemed to us interesting enough to put them into a paper.

The rest of the paper is divided into sections, including Related Work, Edge routing in XJS, Tiling, Conclusion, and Future work.

Let us start with a short review of some relevant to us publications.

## 29 Related work

30 A popular graph drawing tool Graphviz [1] applies method Scalable Force-Directed Placement [2] for large graphs, with no support for tiling. The edge routing for this method builds the whole visibility graph and routes edges on it. This can be very slow because the visibility graph can have  $O(n^2)$  edges, where 31  $n$  is the number of the nodes in the graph. Interestingly, the funnel algorithm [3, 32 4], the last step of our approach, is used in Graphviz for the edge routing in the Sugiyama layout. We are not aware of any tool that integrates Graphviz and 33 uses tiling as well.

34 yWorks [5] has method "Organic edge routing" that produces edge routes around the nodes. We could find only a very general description of the method: 35 "The algorithm is based on a force directed layout paradigm. Nodes act as repulsive forces on edges in order to guarantee a certain minimal distance between 36 nodes and edges. Edges tend to contract themselves. Using simulated annealing, this finally leads to edge layouts that are calculated for each edge separately". 37 It seems the algorithm runs in  $O(n+m)\log(n+m)$  time, where  $n$  is the number of the nodes and  $m$  is the number of the edges.

38 ReGraph [6] uses WebGL as the viewing platform. It can render a large graph using straight lines for the edges. The tool does not support tiling, but instead 39 the user interactively opens the node that is a cluster of nodes.

40 "graph-tool.skewed" [7] does not implement its own layout algorithms or edge routing algorithms, but instead provides a nice wrapper around the algorithms 41 from other layout tools.

42 Circos [8] visualizes large graphs in a circular layout. It does not support 43 tiles.

44 Cosmograph [9] uses a GPU to calculate the layout of a graph and can handle a graph with a million nodes. It renders edges as straight lines. It does 45 not support tiling.

46 The authors of [10] implemented GraphMaps, a tool for large graph visualization. The tool only runs on Windows. The edge were routed as polylines 47 on a triangulation and were not optimized. The tool supported tiling, but the problem of the limiting number of visible entities was not solved.

48 In [11] an approach to visualize a huge graph is described. The method uses tiles and edge bundling following [12], which is applied at the last moment during 49 the graph browsing. The latter calculation is done on the client side. The rest 50 and the majority of the calculations runs on several servers.

## 65 Edge routing in XJS

66 The user study of Xu et al [13] shows that straight edges improve the user comprehension of a graph drawing. From the other hand, Holten et al [14] show 67 that strongly curved edges do not perform well in this regard. In our routing, we 68 try to keep the edges as straight as possible, and to curve them just enough to 69

70 avoid the nodes. Our motivation for developing the routing described here was  
 71 to improve the quality of edges and the algorithm speed.

82 The edge routing starts, as in [15], by building a spanner graph, an approxi-  
 83 mation of the full visibility graph, and then finding the edge routes as shortest  
 84 paths on the spanner. The spanner, see Fig 2, is built on a variation of a Yao  
 85 graph, which was introduced independently by Flinchbaugh, and Jones [16], and  
 86 Yao [17]. This graph is built with a help of a set of cones with the apices at  
 87 the vertices. Each cone of the set has the same angle, usually in the form of  $\frac{2\pi}{k}$ ,  
 88 where  $k$  is a natural number,  $k = 12$  in our settings. The family of cones with  
 89 the apex at a specific vertex partition the plane, as illustrated in Fig. 1. For each  
 90 cone at most one edge is created connecting the cone apex with a vertex inside  
 91 the cone. This way the spanner has at most  $kn$  edges, where  $n$  is the number of  
 92 the vertices. We cover each node by a polygon with a relatively small number of  
 93 corners, at most 8. Polygon corners play role of the vertices of the spanner. As a  
 94 result, the spanner has  $O(N)$  edges, where  $N$  is the number of the graph nodes.

95  
 99 The approach of [15] applies local optimizations to shorten an edge path.  
 100 Namely, it tries to shortcut one vertex at a time from the path, as illustrated in  
 101 Fig 3. To smoothen a path, it fits Bezier segments into the polyline corners by  
 102 using a binary search to find a large fitting segment, see Fig 4.  
 103 We noticed that when the shortcutting of polyline corners fails, the resulting  
 104 path might remain not visually appealing, as shown in Fig. 3. We replace the  
 105 shortcutting with a more precise, but still efficient optimization described below:  
 106 that is one of the main contributions of our work.

## 107 Path optimization

108 We finalize edge routes by a slight modification of the “funnel” algorithm [3, 4],  
 109 routing a path inside a simple polygon, that is a polygon without holes.

110 An application of the ‘path in a simple polygon’ optimization to edge routing  
 111 is not a new idea: the novelty of our work is in how we find the polygon and  
 112 how we use it. The authors of Graphvis used the ‘funnel’ algorithm [18], but  
 113 only for hierarchical layouts, where a simple polygon,  $\mathcal{P}$ , containing the path is  
 114 available. They write: “If  $\mathcal{P}$  does not contain holes ... we can apply a standard  
 115 “funnel” algorithm ... for finding Euclidean shortest paths in a simple polygon”.  
 116 In general case they build the visibility graph which is very expensive for a large  
 117 graph.

118 Here we find the polygon  $\mathcal{P}$  for any layout. We drop the requirement that  
 119  $\mathcal{P}$  is simple. Indeed, to run the “funnel” algorithm one only needs a “sleeve”: a  
 120 sequence of triangles leading from the start to the end of the path, where each  
 121 triangle shares a side with its successor. Let us show how to build polygon  $\mathcal{P}$ ,  
 122 create a sleeve, and produce an optimized path.

123 We call obstacles,  $\mathcal{O}$ , the set of polygons covering the original nodes, see  
 124 Fig. 2. Before routing edges, we calculate a Constrained Delaunay Triangula-  
 125 tion [19] on  $\mathcal{O}$ , following [20]. Let us call this triangulation  $\mathcal{T}$ .

126 For each edge of the graph we proceed with the following steps.



**Fig. 1.** Yao graph

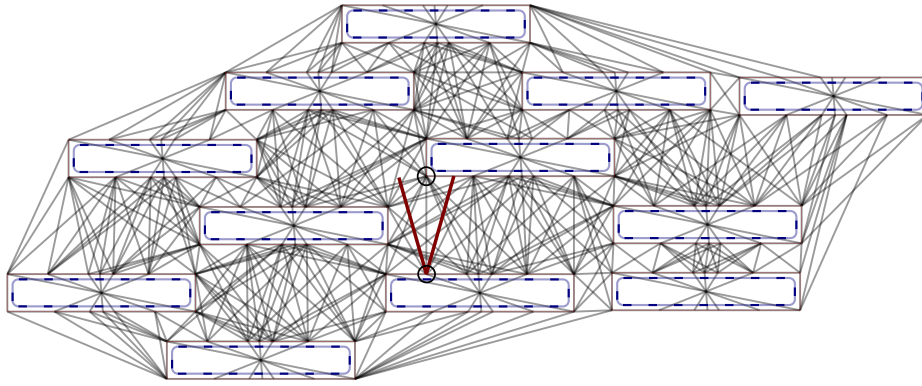


**Fig. 2.** Spanner graph is built using the idea of Yao graphs. The dashed curves are the original node boundaries. Each original curve is surrounded by a polygon with some offset to allow the polyline paths smoothing without intersecting the former. The edge marked by the circles is created because the top vertex is inside the cone, and it is the closest among such vertices to the cone apex. The apex of the cone is the lower vertex of the edge. XJS uses cone angle  $\frac{\pi}{6}$ , so the edges of the spanner can deviate from the optimal direction by this angle. Therefore, the shortest paths on the spanner have length that is at most the optimal shortest length multiplied by  $\frac{1}{\cos(\frac{\pi}{6})} \simeq 1.155$ .



**Fig. 3.** Unsuccessful shortcut

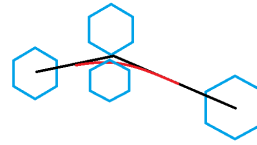
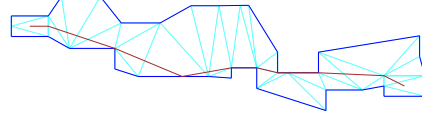


**Fig. 4.** Fitting a Bezier segment into a polyline corner



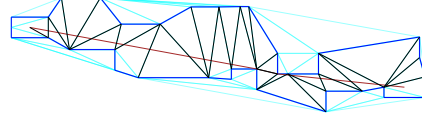
127 **Fig. 5.** Path  $\mathcal{L}$  with  $\mathcal{T}$ , a fragment.



128 **Fig. 6.** Polygon  $\mathcal{P}$  containing  $\mathcal{L}$ .



129 **Fig. 7.** New triangulation of  $\mathcal{P}$ .



130 **Fig. 8.** The optimized path together  
131 with the sleeve diagonals.

134 We route a path, called  $\mathcal{L}$ , on the spanner, as illustrated by Fig. 5. Let  $\mathcal{S}$   
135 and  $\mathcal{E}$  be the obstacles containing, correspondingly,  $\mathcal{L}$ 's start and end point.  
136 To obtain  $\mathcal{P}$ , let us consider  $\mathcal{U}$ , the set of all triangles  $t \in \mathcal{T}$  such that either  
137  $t \subset \mathcal{S} \cup \mathcal{E}$ , or  $t$  intersects  $\mathcal{L}$  and is not inside any obstacle in  $\mathcal{O} \setminus \{\mathcal{S}, \mathcal{E}\}$ . The  
138 union of  $\mathcal{U}$  gives us  $\mathcal{P}$ . The boundary of  $\mathcal{P}$  comprises all sides  $e$  of the triangles  
139 from  $\mathcal{U}$  such that  $e$  belongs to exactly one triangle from  $\mathcal{U}$ , see Fig. 6.

140 To create the sleeve [3, 4], we need to have a triangulation of  $\mathcal{P}$  such that every  
141 edge of the triangulation is either a boundary edge of  $\mathcal{P}$ , or a diagonal of  $\mathcal{P}$ .  
142 Because  $\mathcal{U}$  might not have this property, as in Fig. 6, we create a new Constrained  
143 Triangulation of  $\mathcal{P}$ , where the set of constrained edges is the boundary of  $\mathcal{P}$ , see  
144 Fig. 7.

145 We trace path  $\mathcal{L}$  through the new triangulation and obtain the sleeve. Finally,  
146 we apply the funnel algorithm on the sleeve and obtain the path which is the  
147 shortest in the homotopy class of  $\mathcal{L}$ , as illustrated in Fig. 8.

148 The discussion [21] of the algorithm helped us in the implementation of the  
149 funnel algorithm.

150 Polygon  $\mathcal{P}$  is not necessarily simple, as shown in Fig. 9. In this example the  
151 path that we calculate with the funnel algorithm is not the shortest path inside  
152  $\mathcal{P}$ .

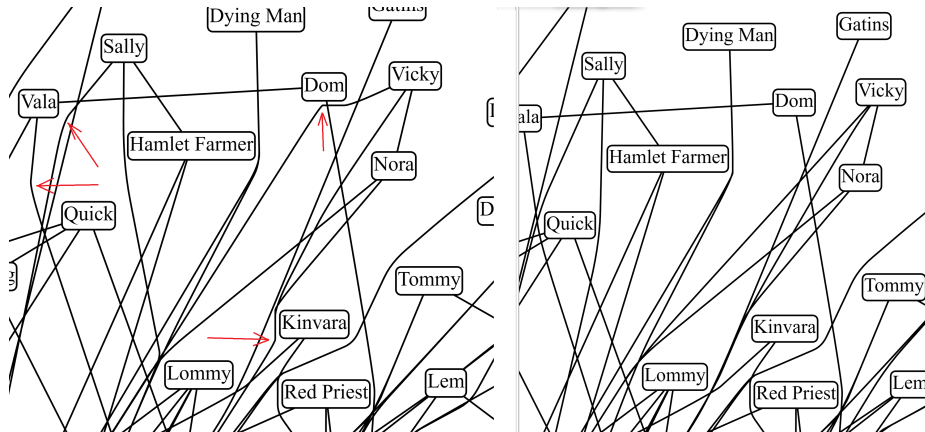
## 153 Performance and quality comparison

157 In Fig. 10 we compare the paths generated by the old and the new method. We  
158 can see that the paths produced by the new method have no kinks. We also know  
159 that these paths are the shortest in their 'channels'. Arguably, the new method  
160 produces better paths.

161 Our performance experiments are summarized in Table. 1. We see that the  
162 older approach outperforms the new one on the smaller graphs; those with the  
163 number of nodes under 2000. The new method is faster on the rest of the graphs.



132 **Fig. 9.**  $\mathcal{P}$  is not simple. The dotted path is shorter than the dashed one that  
 133 was found by the routing.



154 **Fig. 10.** Comparing the old, on the left, and the new, on the right, paths. The  
 155 arrows on the left fragment point to the kinks that were removed by the new  
 156 method.

164 We prefer the new method regardless of the graph size because it provides better  
 165 path quality and the slowdown is insignificant.

graph	nodes	edges	old method's time	new time
social network [22]	407	2639	1.0	1.4
b103 [23]	944	2438	1.6	2.0
b100 [24]	1463	5806	5.6	5.785
composers [25]	3405	13832	510.5	20.3
p2p-Gnutella04 [26]	10876	39994	375.4	304.2
facebook_combined [27]	4039	88234	132.2	123.7
lastfm_asia_edges [28]	7626	27807	43.3	54.7
deezer_europe_edges [28]	28283	92753	1596.9	1402.6
ca-HepPh [29]	12008	237010	521.2	495.0

**Table 1.** Performance comparison with time in seconds.

## 177 1 Tiling

178 We had two goals when working on tiling. The first goal was to make exploring  
 179 the graph in our tool similar to using online maps. The second goal was efficiency.  
 180 The algorithm works in three phases. The first phase builds the levels starting  
 181 from the lowest level and proceeding to higher and more detailed levels, with  
 182 smaller tiles, until no more tile subdivision is required. The second phase filters  
 183 out the entities from the layers to satisfy the capacity quota, as in [10]. Finally,  
 184 the third phase simplifies the edge routes to utilize the space freed by the filtered  
 185 out entities.

186 A tile, in our settings, is a pair  $(rect, tiledata)$ , where  $rect$  is the rectangle of  
 187 the tile and  $tiledata$  is a set of *tile elements* visible in  $rect$ . A *tile element* could  
 188 be a node, an edge label, an edge arrowhead, or an *edge clip*. An edge clip is a  
 189 pair  $(e, p)$ , where  $e$  is an edge and  $p$  is a continuous piece of the edge curve  $c_e$ .  
 190 Sometimes we need several edge clips to trace an edge through a tile.

191 The initial tile, the only tile on level 0, is represented by pair  $(0, 0)$ . For  
 192  $z = 1$ , there are four tiles:  $(0, 0)$ ,  $(0, 1)$ ,  $(1, 0)$ , and  $(1, 1)$ . Each tile  $(i, j)$  can be  
 193 subdivided into four sub-tiles for level  $z + 1$ :  $(2i, 2j)$ ,  $(2i, 2j + 1)$ ,  $(2i + 1, 2j)$ , and  
 194  $(2i + 1, 2j + 1)$ .

195 Each  $z$ -level is represented by a map  $L_z$ , so  $L_z(i, j)$  gives us a specific tile.  
 196 Empty tiles correspond to undefined  $L_z(i, j)$ .

197 We use edge clips to represent the edge intersections with the tiles and provide  
 198 the renderer with the minimal geometry that is sufficient to render a tile. To  
 199 achieve this we require property  $\mathcal{F}$ :

200 a) For each tile  $t$ , for each edge clip  $(e, p) \in t.tiledata$ , we have:  $p \subset t.rect$   
 201 and  $p$  might cross the boundary of the  $t.rect$  only at endpoints of  $p$ .

202       b) For each edge  $e$  we have : the union of all  $p$  for all  $(e, p) \in t.tiledata$  is  
 203 equal to  $c_e \cap t.rect$ .

#### 204 **First phase of tiling**

205 The first phase starts with  $L_0 = \{(0, 0) \rightarrow (rect, tiledata)\}$ : and *tiledata* comprising  
 206 edge clips  $(e, c_e)$ , for all edges  $e$  of the graph, all graph nodes, all edge labels,  
 207 and all edge arrowheads. We ensure property  $\mathcal{F}$  by setting *rect* to a padded  
 208 bounding box of the graph, so each edge curve does not intersect the boundary  
 209 of *rect*.

210 Let us assume that  $L_z$  is already constructed and  $\mathcal{F}$  holds for its tiles. To  
 211 build level  $L_{z+1}$  we divide each tile  $t = L_z(i, j)$  into four sub-tiles of equal size.  
 212 For each node, arrowhead, or edge label of *t.tiledata*, if the bounding box of the  
 213 element intersects the sub-tile's rectangle then we add the element to the sub-tile  
 214 *tiledata*.

215 The edge clip treatment is more involved. Let  $(e, p)$  be an edge clip belonging  
 216 to tile  $t$ . We find all intersections of curve  $p$  with the horizontal midline and the  
 217 vertical midline of *t.rect*. Each intersection can be represented as  $p[t_j]$ . We sort  
 218 sequence  $u = [start, \dots, t_j, \dots, end]$ , where  $[start, end]$  is the parameter domain  
 219 of  $p$ , in ascending order, and remove the duplicates.

220 Next we create edge clips  $(e, l_k) = (e, trim(p, u_k, u_{k+1}))$ , as shown in Fig 11.  
 221 We assign each edge clip  $(e, l_k)$  to the sub-tile with the rectangle containing the  
 222 bounding box of  $l_k$ .

223 Because, by the induction assumption property  $\mathcal{F}$  is true on  $L_z$ , and by  
 224 construction, each new edge clip can cross the boundary of the sub-tile only at  
 225 the clip endpoints. We also cover all the intersections of  $p$  with the sub-tiles with  
 226 the new edge clips, so the property  $\mathcal{F}$  holds for  $L_{z+1}$ .

227 Two parameters control the algorithm: tile capacity,  $\mathcal{C}$ , and the minimal size  
 228 of a tile:  $(\mathcal{W}, \mathcal{H})$ . If for each  $(i, j)$  the number of elements in  $L_z(i, j).tiledata$   
 229 is not greater than  $\mathcal{C}$ , and if  $w \leq \mathcal{W}$  and  $h \leq \mathcal{H}$ , where  $(w, h)$  is the current  
 230 tile size, then we try to build the next level  $L_{z+1}$ . Otherwise, the second phase  
 231 starts.

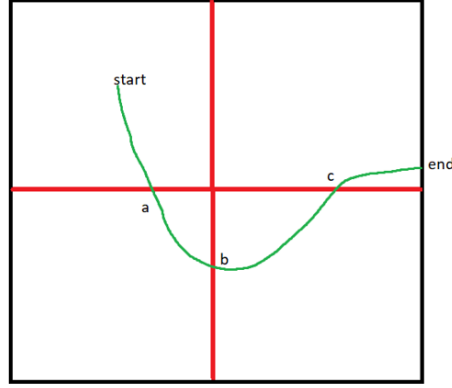
232 In our setting  $\mathcal{C} = 500$ , and  $(\mathcal{W}, \mathcal{H}) = 3(w, h)$ , where  $w$  is the average width  
 233 and  $h$  is the average height of the nodes of the graph.

234 For efficiency, we do not create a new curve in an edge clip but keep two  
 235 parameters indicating the clipped segment start and end. A possible optimization  
 236 here is to find the repeated segments in the edge curves that naturally appear  
 237 while routing through the same graph with the same algorithm, and reuse the  
 238 repeated segment to save memory and to avoid the same calculation in edge  
 239 clipping.

#### 244 **Second phase of tiling**

245 In this phase, some entities from the lower levels are filtered out. We do not  
 246 change the highest, the most detailed level. We sort the nodes of the graph into





223 **Fig. 11.** Intersect curve  $[start, end]$  with the midlines. Sort the intersections pa-  
 224 rameters, together with start and end, into array  $u = [start, a, b, c, end]$ . Split the  
 225 curve to sub-curves  $[start, a]$ ,  $[a, b]$ ,  $[b, c]$ , and  $[c, end]$ . Each sub-curve is confined  
 226 to a single sub-tile.

247 array  $N$  by PageRank [30]. For each level  $L$ , except of the highest, we proceed  
 as follows.

---

```

1: procedure FILTER( $L$ )
2:    $r \leftarrow \text{removeEntities}(L)$ 
3:   for all  $n$  in  $N$  do
4:     if ! $\text{addNodeToLevel}(n, r, N)$  then break
5:   end if
6: end for
7: end procedure

```

---

248  
 249 Here  $\text{removeEntities}(L)$  empties all the tiles of level  $L$ , and returns map  $r$  al-  
 250 lowing to restore the tiles. Map  $r$  maps each graph element to an array of tile  
 251 elements representing it in  $L$ . Function  $\text{addNodeToLevel}(n)$  tries to add node  $n$   
 252 to  $L$ , it also tries to add the tile elements for self edges of  $n$ , and the tile elements  
 253 for the edges connecting  $n$  with the nodes ranked at least as high as  $n$ . These  
 254 nodes are the nodes already added to  $L$ .

255 This procedure guarantees that each tile of  $L$  has no more than  $\mathcal{C}$  elements.

### 256 **Third phase of tiling**

257 In the third phase we use the fact that some nodes are not present on the  
 258 level. For all levels, except of the highest, we reroute the edges but only around  
 259 the nodes that are present in the level. We do not calculate edge routes from  
 260 scratch, but use the existing routes and only apply the "funnel" heuristic in

261 larger channels. This gives us simpler edge routes but still has the visual stability  
262 during the level change while browsing.

## 263 2 Conclusion

264 The first contribution is an efficient edge routing algorithm. The algorithm re-  
265 places each polyline path with the shortest path that does not intersect the  
266 nodes and stays in the polyline homotopy class, the channel, and then produces  
267 the smooth composite curve. It uses a modification of the 'funnel' in the simple  
268 polygon algorithm, where we drop the requirement that the polygon is simple.

269 We described the scenario where the graph spanner is used. Instead, our  
270 approach can start with any routing with polylines outside the nodes.

271 The algorithm is fast and creates visually pleasing results.

272 The tiling method is the second contribution of this study. It allows large  
273 graphs to be visualized in a web browser, similar to online maps. The method  
274 provides an overview of the most important nodes and edges of the graph by  
275 making them visible on the top levels while keeping the number of visible el-  
276 ements under a given limit. The novelty of the method is that it efficiently  
277 subdivides the edges by using the tiles, and simplifies the edges on the upper  
278 levels with the edge routing algorithm mentioned above.

## 279 3 Future work

- 280 – Find a tiling method that guarantees that each tile has no more than  $\mathcal{C}$  el-  
281 ements on every level. One approach is to use more aggressive, and regular  
282 edge bundling to reduce the number of edge clips in the tiles.
- 283 – Our tile calculation is memory intensive and takes a longer time for larger  
284 graphs. The largest graph from the Table 1 that we were able to load with  
285 Chrome, and Edge using the tiling procedure was p2p-Gnutella04 [26]. One  
286 of the reasons was the memory limit on a process in those browsers, another  
287 was the long running-time of the tiling procedure. A possible measure would  
288 be saving the tiles to the disk and loading them on demand.
- 289 – For the user convenience we would like to run the layout, routing, and tiling,  
290 in a worker thread to avoid blocking the main thread.
- 291 – Addressing node labels visibility is an important task. We would like to en-  
292 large the most important nodes of the view so that their labels are readable.

## 293 References

- 294 1. “Graphviz.” <http://www.graphviz.org/>.
- 295 2. “sfdp.” <https://graphviz.org/docs/layouts/sfdp/>.
- 296 3. B. Chazelle, “A theorem on polygon cutting with applications,” in *23rd Annual*  
297 *Symposium on Foundations of Computer Science (sfcs 1982)*, pp. 339–349, IEEE,  
298 1982.

- 299 4. J. Hershberger and J. Snoeyink, "Computing minimum length paths of a given  
300 homotopy class," *Computational geometry*, vol. 4, no. 2, pp. 63–97, 1994.
- 301 5. "yworks." <https://yworks.com/products/yed>.
- 302 6. "Regraph." <https://cambridge-intelligence.com/regraph/>.
- 303 7. "Skewed." <https://graph-tool.skewed.de>.
- 304 8. "Circos." <http://circos.ca/>.
- 305 9. "Cosmograph." <https://cosmograph.app>.
- 306 10. L. Nachmanson, R. Prutkin, B. Lee, N. H. Riche, A. E. Holroyd, and X. Chen,  
307 "Graphmaps: Browsing large graphs as interactive maps," in *Graph Drawing and*  
308 *Network Visualization: 23rd International Symposium, GD 2015, Los Angeles, CA,*  
309 *USA, September 24-26, 2015, Revised Selected Papers 23*, pp. 3–15, Springer, 2015.
- 310 11. A. Perrot and D. Auber, "Cornac: Tackling huge graph visualization with big data  
311 infrastructure," *IEEE Transactions on Big Data*, vol. 6, no. 1, pp. 80–92, 2018.
- 312 12. C. Hurter, O. Ersoy, and A. Telea, "Graph bundling by kernel density estimation,"  
313 in *Computer graphics forum*, vol. 31, pp. 865–874, Wiley Online Library, 2012.
- 314 13. K. Xu, C. Rooney, P. Passmore, D.-H. Ham, and P. H. Nguyen, "A user study  
315 on curved edges in graph visualization," *IEEE transactions on visualization and*  
316 *computer graphics*, vol. 18, no. 12, pp. 2449–2456, 2012.
- 317 14. D. Holten and J. J. Van Wijk, "A user study on visualizing directed edges in  
318 graphs," in *Proceedings of the SIGCHI conference on human factors in computing*  
319 *systems*, pp. 2299–2308, 2009.
- 320 15. T. Dwyer and L. Nachmanson, "Fast edge-routing for large graphs," in *Graph*  
321 *Drawing: 17th International Symposium, GD 2009, Chicago, IL, USA, September*  
322 *22-25, 2009. Revised Papers 17*, pp. 147–158, Springer, 2010.
- 323 16. B. Flinchbaugh and L. Jones, "Strong connectivity in directional nearest-neighbor  
324 graphs," *SIAM Journal on Algebraic Discrete Methods*, vol. 2, no. 4, pp. 461–463,  
325 1981.
- 326 17. A. C.-C. Yao, "On constructing minimum spanning trees in k-dimensional spaces  
327 and related problems," *SIAM Journal on Computing*, vol. 11, no. 4, pp. 721–736,  
328 1982.
- 329 18. D. P. Dobkin, E. R. Gansner, E. Koutsofios, and S. C. North, "Implementing a  
330 general-purpose edge router," in *Graph Drawing: 5th International Symposium,*  
331 *GD'97 Rome, Italy, September 18–20, 1997 Proceedings 5*, pp. 262–271, Springer,  
332 1997.
- 333 19. B. Delaunay *et al.*, "Sur la sphere vide," *Izv. Akad. Nauk SSSR, Otdelenie Matem-*  
334 *aticheskii i Estestvennyka Nauk*, vol. 7, no. 1, pp. 793–800, 1934.
- 335 20. V. Domiter and B. Žalik, "Sweep-line algorithm for constrained delaunay triangulation," *International Journal of Geographical Information Science*, vol. 22, no. 4,  
336 pp. 449–462, 2008.
- 337 21. "Funnel algorithm." <https://page.mi.fu-berlin.de/mulzer/notes/alggeo/polySP.pdf>.
- 338 22. A. Beveridge and M. Chemers, "The game of game of thrones: Networked concordances and fractal dramaturgy," in *Reading Contemporary Serial Television*  
339 *Universes*, pp. 201–225, Routledge, 2018.
- 340 23. "b103." [https://github.com/microsoft/automatic-graph-](https://github.com/microsoft/automatic-graph-layout/blob/master/GraphLayout/Test/MSAGLTests/Resources/DotFiles/LevFiles/b103.dot)  
341 [layout/blob/master/GraphLayout/Test/MSAGLTests/Resources/DotFiles/LevFiles/b103.dot](https://github.com/microsoft/automatic-graph-layout/blob/master/GraphLayout/Test/MSAGLTests/Resources/DotFiles/LevFiles/b103.dot).
- 342 24. "b100." [https://github.com/microsoft/automatic-graph-](https://github.com/microsoft/automatic-graph-layout/blob/master/GraphLayout/Test/MSAGLTests/Resources/DotFiles/LevFiles/b100.dot)  
343 [layout/blob/master/GraphLayout/Test/MSAGLTests/Resources/DotFiles/LevFiles/b100.dot](https://github.com/microsoft/automatic-graph-layout/blob/master/GraphLayout/Test/MSAGLTests/Resources/DotFiles/LevFiles/b100.dot).
- 344 25. "Skewed." <http://mozart.diei.unipg.it/gdcontest/contest2011/composers.xml>.
- 345 26. "p2p-gnutella04." <https://snap.stanford.edu/data/p2p-Gnutella04.html>.
- 346 27. "facebookcombined." [https://snap.stanford.edu/data/facebook\\_combined.txt.gz](https://snap.stanford.edu/data/facebook_combined.txt.gz).

- 349 28. B. Rozemberczki and R. Sarkar, “Characteristic Functions on Graphs: Birds of a  
350 Feather, from Statistical Descriptors to Parametric Models,” in *Proceedings of the*  
351 *29th ACM International Conference on Information and Knowledge Management*  
352 *(CIKM '20)*, p. 1325–1334, ACM, 2020.
- 353 29. J. Leskovec, J. Kleinberg, and C. Faloutsos, “Graph evolution: Densification  
354 and shrinking diameters,” *ACM transactions on Knowledge Discovery from Data*  
355 *(TKDD)*, vol. 1, no. 1, pp. 2–es, 2007.
- 356 30. L. Page, S. Brin, R. Motwani, and T. Winograd, “The pagerank citation ranking:  
357 Bringing order to the web,” *Stanford InfoLab*, vol. 249, no. 373, pp. 1–17, 1999.